Observation of the dynamic Stark effect on electromagnetically induced transparency

Changjiang Wei* and Neil B. Manson†
Laser Physics Center, The Australian National University, Canberra, Australian Capital Territory 0200, Australia
(Received 21 April 1999)

Using electron-spin-resonance transitions within the nitrogen-vacancy center in diamond, we have obtained a sharp electromagnetically induced transparency (EIT) feature when the coupling and probing fields satisfy a two-photon resonance condition. In this paper it is shown that by the application of an additional driving field the sharp EIT feature can be split into a doublet or a triplet depending on the experimental configuration. The results are interpreted in terms of dynamic Stark splitting of the EIT feature, and the spectra are shown to be related to Autler-Townes and Mollow spectra. [S1050-2947(99)10209-9]

PACS number(s): 42.50.−p, 42.62.Fi

I. INTRODUCTION

Due to intriguing physics and potential applications, there has been considerable interest in the study of electromagnetically induced transparency (EIT) [1–8]. A simple situation to consider is a three-level atom interacting with a coupling and a probing field and transparency can be attained in a V, Λ, or Ξ configuration. Here we concentrate on a Λ three-level atom consisting of an upper level and two lower levels. The upper level is coupled to the two lower levels by coupling and probing fields, and the induced transparency occurs when the difference in frequencies of the two fields matches the transition frequency between the two lower levels. When the transition between the two lower levels is narrow, the EIT feature is likewise narrow. This is frequently the situation when the upper level is at an optical frequency and the separation of the two lower levels (corresponding to hyperfine levels) is in the radio or microwave frequency region.

In this paper we present investigations of EIT in a Λ-type system. The system is different from earlier systems in that the EIT is associated with electron-spin-resonance (ESR) transitions rather than optical transitions. The upper level is associated with an electron-spin level, and the two lower levels are hyperfine levels both associated with the second electron-spin level [9]. There are parallels between this situation and an optical Λ systems, but electric-dipole-allowed transitions between electronic states in the optical case are replaced by magnetic-dipole-allowed transitions between spin levels in the ESR case. The advantage of studying such a system is that it is reasonably straightforward to drive or probe three transitions associated with the Λ three-level system using similar experimental techniques. This is a very different situation as that encountered with optical EIT phenomenon, where entirely different experimental techniques would be required to study the optical and hyperfine transitions. Being able to make such a study enables us to obtain a better understanding of the associated phenomenon.

The EIT feature associated with magnetic-resonance transitions has been reported by other research workers [8]. In this previous report of EIT, a pulsed excitation and detection technique was adopted to obtain the absorption of a probing field in the presence of a coupling field. The EIT feature was, hence, inferred from time domain measurements. In our work the EIT is investigated using frequency domain measurements in a similar way to that the EIT is usually investigated in the optical spectral region. This permits an easier comparison between the present investigation and previous optical work. The frequency domain measurements of the resonance transitions is achieved using the Raman heterodyne method [10]. In this scheme a rf field is applied to the sample, but the electron-spin transitions and the hyperfine transitions are detected as rf beat signals between a laser field and a stimulated optical field, and the magnitude of the beat signal gives a measure of the absorption at that rf frequency. With this technique continuous-wave measurement of the weak probing field absorption spectrum becomes possible even in the presence of strong-coupling field, and, as there is no need to use a resonant coil, it is possible to sweep the probing field to obtain the frequency dependence of the absorption and dispersion. The sample used in the present investigation is a diamond containing nitrogen-vacancy (N-V)centers. With this center we have control over the frequency of the electron-spin transitions, and to a lesser extent the frequency of the hyperfine transitions as well as the associated dephasing rate [11,12]. The ESR transition frequency can be set in the 50–80-MHz frequency range and the hyperfine transition frequency at 4–6 MHz, and with these frequencies we are able to study all the transitions associated with the EIT feature without the need of changing the experimental arrangements [9]. The Raman heterodyne detection scheme also has very good sensitivity in this frequency region, and permits us to make sensitive measurements of the EIT spectrum under various experimental conditions.

In early investigations of the N-V center we studied the dynamic Stark effect [13,14] associated with the hyperfine transitions, and reported both Mollow [15] and Autler-Townes [16] spectra. The hyperfine levels involved here are precisely those associated with the previous study and we take advantage of this fact to investigate how the EIT is changed when the hyperfine transitions are driven as previously by a strong field. It is found that the driving field modifies the EIT spectrum, and we show that there are parallels with the Autler-Townes and Mollow spectra. The ob-

*Electronic address: changjiang.wei@anu.edu.au
†Electronic address: neil.manson@anu.edu.au

servation illustrates interesting dynamics of an EIT feature subjected to a strong driving field. These measurements are all associated transitions in the rf spectral region, and as a consequence there is little likelihood for applications. However, it can be anticipated that equivalent observations may be made for EIT features in the optical spectral region. Our results may indicate a way of manipulating the EIT in the optical region, such as opening multiple EIT window or frequency tuning of the EIT feature.

There are up to five electromagnetic fields involved in the present work, and to avoid confusion we introduce notations to distinguish different fields. The experiment involves optical detection, and for this there is both a weak laser field and a stimulated optical Raman field. These two fields are solely involved with the detection and not involved in the generation and modification of the EIT feature. These optical fields will only be mentioned in the discussion of the experimental techniques. The more significant fields are all in the rf region of the spectrum. The observation of an EIT feature involves two rf fields and the splitting of the EIT feature involves a third lower-frequency rf field. The transparency is induced by a fixed frequency ''coupling'' field ω_c and is observed by a swept frequency ''probing'' field ω_p. The response at the frequency of the probing field ω_p is monitored, and gives the reported spectrum. The term ''driving'' field is used to refer to the additional or the third rf field applied at lower frequency ω_d. It is this extra rf field that gives rise to the splitting of the EIT feature which is the focus of this paper.

II. EXPERIMENT

The experiment involves ESR transitions within the ground state of the N-V center in diamond, and the magnetic resonance is detected optically using the Raman heterodyne method. The N-V center in diamond consists of a substitutional nitrogen atom and a vacancy at the nearest-neighbor carbon site and has a C_{3v} symmetry, with the C_3 axis lying along the [111] crystallographic direction [17]. The optical zero-phonon line at 638 nm utilized in the Raman heterodyne is due to an $^3A \rightarrow {}^3E$ transition [18]. The ^3A ground state is an electron-spin triplet, and the crystal-field interaction splits the spin triplet into a spin singlet $S_Z=|0\rangle$ and a spin doublet $S_Z=|\pm 1\rangle$ with a separation of 2.88 GHz. A static magnetic field applied along the principle axis of the N-V center lifts the degeneracy of the $S_Z=|\pm 1\rangle$ levels and gives a linear Zeeman splitting of the $S_Z=|\pm 1\rangle$ spin levels. Due to the Zeeman splitting the $S_Z=|-1\rangle$ spin level approaches the $S_Z=|0\rangle$ spin level, and for a dc magnetic field of 0.1028 T there is an avoided crossing of these levels. The experiments are carried out with a static magnetic field close to the avoided crossing value such that the $S_Z=|0\rangle \rightarrow |-1\rangle$ transition frequency is in the range of 50–80 MHz [Fig. 1(a)]. There is a hyperfine interaction associated with the ^{14}N nuclei ($I=1$), and as a result each of the electron-spin levels has three hyperfine components and the hyperfine transition frequencies are of the order of a few MHz. With such frequencies the ESR and hyperfine transitions can be conveniently detected using the same photodiode, and the rf fields can be supplied using the same nonresonance rf coil. Also in the region of the level anticrossing, there is a significant mixing of the spin states due to both hyperfine interaction

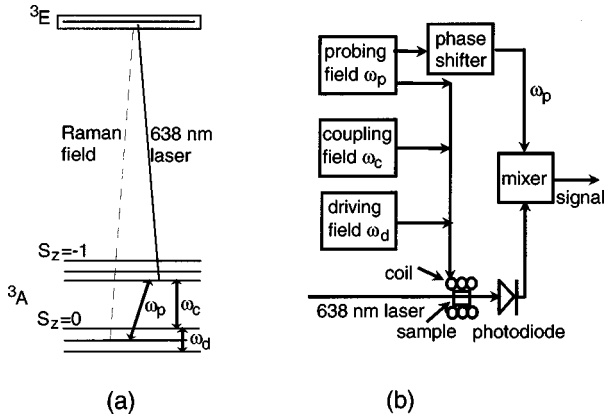

FIG. 1. (a) Energy-level diagram illustrating processes involved in Raman heterodyne detection of magnetic resonance and splitting of the EIT feature. The ESR spectrum as probed by a rf probe field ω_p is measured through a beating signal between laser and Raman optical fields. Applying a coupling field ω_c induces an EIT feature in the spectrum of the probe field ω_p, and the driving field ω_d causes a splitting of this EIT feature. (b) Schematic of the experimental setup.

and off-axis Zeeman interaction, and there are several consequences of this wave-function mixing. The three ESR transitions in which nuclear-spin projection is conserved dominate the ESR spectrum, but with the spin mixing some additional transitions involving a nominal change of nuclear-spin state become weakly allowed. These extra transitions are important, as in the EIT experiments the coupling fields are usually introduced to be resonant with these weakly allowed transitions. There are also significant changes to the strength of the hyperfine transitions. In this case the hyperfine transitions between nuclear-spin levels take on some electron-spin character, and as a consequence the oscillator strengths can be enhanced by up to a factor of 100. The enhancement means that it is possible to obtain strong effective driving fields while using only modest rf field strength (<1 G), and this facilitates splitting of the EIT feature. The frequencies of all transitions are susceptible to alignment and the magnitude of the applied dc magnetic field. Small movements of the sample upon the temperature recycling and minor variation of the magnetic-field magnitude can lead to minor changes from day to day in the linewidth of the hyperfine transitions and changes in the ESR and hyperfine transition frequencies. This is not of concern as transition frequencies, and other relevant parameters can all be measured as required. In fact some variation of the parameters can become an advantage for allowing us to verify the correlation between the properties of the EIT feature and those of hyperfine transitions.

The Raman heterodyne detection of magnetic resonance relies on a three-level optical rf double-resonance process. An rf field ω_p couples the spin levels, and a laser field couples one of the spin levels (say, the $S_Z=|-1\rangle$ level) to the optical excited level ^3E. As indicated in Fig. 1(a), these two coherent fields stimulate a coherent field in the remaining optical transition between level $S_Z=|0\rangle$ and the same ^3E level. The stimulated Raman optical field beats with the transmitted laser field at the rf frequency ω_p, and is detected using a photodiode. This beating signal reflects the coherence in the ESR transition. By sweeping the probe rf fre-

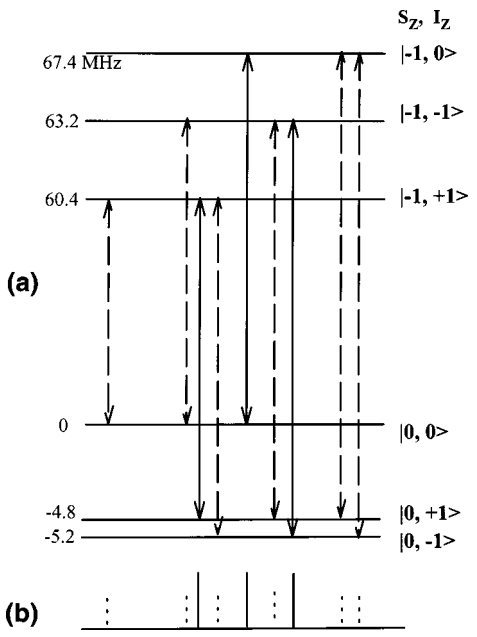

FIG. 2. (a) Energy-level diagram of the electron-spin levels and hyperfine levels of the N-V center for a dc magnetic field of ~0.106 T and a misalignment of ~0.5°. This corresponds to a situation just below the level anticrossing value, which results in the energy value as given in the figure. The solid vertical arrows show three allowed ESR transitions, and the dashed vertical arrows indicate the nominally forbidden ESR transitions. (b) Schematic of the ESR spectrum.

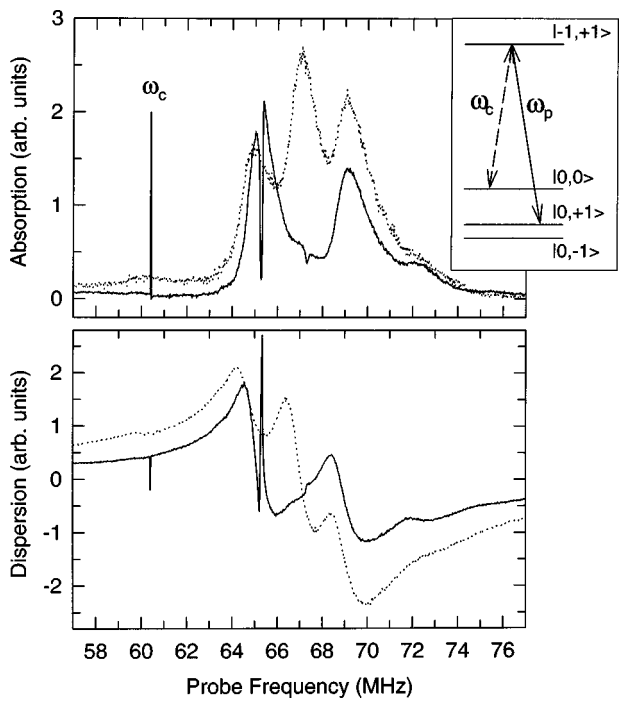

FIG. 3. The dotted trace gives the ESR absorption (upper) and dispersion (lower) spectra measured by the Raman heterodyne technique using a weak swept probe field. A schematic of this spectrum has been given in Fig. 2(b). The solid trace gives the absorption (upper) and dispersion (lower) spectra when a coupling field is introduced at 60.4 MHz; the pickup indicates its position within the spectrum. The EIT feature occurs 4.8 MHz above the coupling field frequency. The energy levels involved in the EIT are given in the inset. Although not discussed in the text, there is also a weak EIT feature at 67.3 MHz associated with a hyperfine separation of 6.9 MHz in the upper electron-spin level.

quency ω_p through the ESR transition, the profile of the magnetic resonance transition can be obtained, and it is this response that is presented in all the experimental traces.

A simplified schematic experimental arrangement is shown in Fig. 1(b). The diamond crystal was mounted in the center of a rf coil located in the bore of a superconducting magnet, and cooled to liquid-helium temperature. The diamond crystal can be rotated within the rf coil to obtain an alignment of the magnetic field to within 1° of the [111] direction, and the magnitude of the dc magnetic field is adjusted to make the system close to the level anticrossing region. A laser beam of 10–20 mW from a Coherent CR-599-21 cw single mode dye laser was tuned to the optical zero-phonon line of the $^3A \rightarrow {}^3E$ transition at 638 nm. The Raman heterodyne signal in the light transmitted through the crystal was detected by a photodiode which has a component in phase and one out of phase with the rf field corresponding to real and imaginary parts of the rf coherence, respectively [10]. When detected in phase or out of phase with the applied rf field, a dispersion or absorption profile of the ESR transition is obtained. As the magnetic resonance is detected through the beating of two optical fields rather than directly through the rf field absorption, it can measure the response of a weak probing field ω_p in the presence of other strong fields such as the coupling rf field ω_c and driving rf field ω_d.

III. RESULTS AND DISCUSSION

As described in Sec. II, the ESR transition studied here is the $S_Z = |0\rangle \rightarrow |-1\rangle$ transition. Due to the nuclear spin $I = 1$ of the nitrogen, each of the electron-spin levels have three hyperfine levels, and hence there are a total of nine possible transitions as illustrated in Fig. 2. As already stated, the three transitions conserving the nuclear-spin project are the strongest, and give rise to the dominant three peaked structure in the Raman heterodyne-detected ESR spectrum (Fig. 3). The absorption and dispersion spectra are shown by the dotted line in the upper and lower traces. The other six transitions are forbidden to first order, but become weakly allowed due to the spin-wave function mixing when the system is close to the avoided crossing and some can be seen in the wings of the spectra.

When a coupling field is applied to the nominal forbidden transitions, sharp EIT features are induced in one of the allowed transitions. By applying the coupling field at various frequencies, EIT features can be observed in all three allowed ESR transitions, and this has been shown in a previous publication [9]. In this paper we restrict our attention to some specific examples. In the first example the coupling field interacts with a weakly allowed transition on the low-energy side of the ESR spectrum corresponding to the $|0,0\rangle \rightarrow |-1,+1\rangle$ transition (Fig. 2). The coupling field induces a narrow transparency feature in the lowest-energy components of the three strong ESR lines corresponding to the $|0,+1\rangle \rightarrow |-1,+1\rangle$ transition (see Fig. 3). This feature has been shown to be narrower than the homogeneous linewidth of the ESR transition, and is readily established to be an EIT

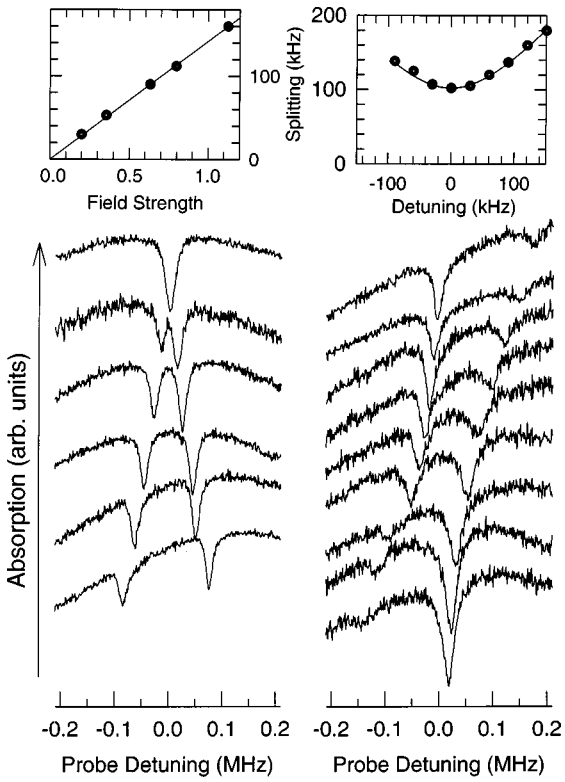

FIG. 4. The effect of a driving field on the EIT feature. The EIT feature is associated with the 4.8-MHz hyperfine splitting (as in Fig. 3), and the driving field is applied at the frequency of the hyperfine transition at 5.2 MHz. In the left-hand traces a resonant driving field is applied and its strength increases, whereas in the right-hand traces the strength of the driving field is fixed and its frequency is varied. The position of the EIT feature in the absence of a driving field is defined as zero frequency. The magnitude of the EIT splitting is measured and plotted in the inset figures. The splitting as a function of driving field Rabi frequency and detuning is given by $\Omega=\sqrt{\chi^2+\delta^2}$, where χ is the (resonant) Rabi frequency and δ is the detuning.

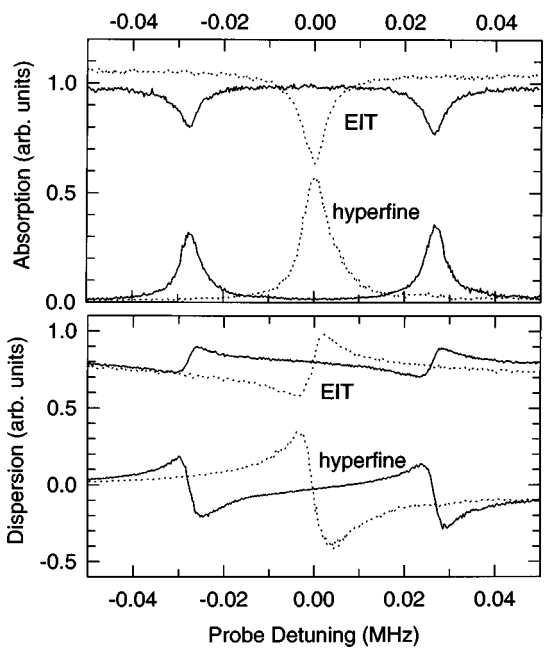

FIG. 5. Absorption (upper) and dispersion (lower) spectrum showing correspondence between the 4.8-MHz hyperfine transition and a corresponding EIT feature. For the hyperfine transition the dotted trace gives the response when there is no driving field, and for the EIT feature the dotted trace gives the response when there is a coupling field but no driving field. For convenience both peak positions are denoted as zero frequency. The solid lines give the corresponding responses when there is a driving field with a Rabi frequency of 54 kHz resonant with the 5.2-MHz transition. For the hyperfine transition this is an Autler-Townes splitting, and there is an exact correspondence between both splitting and linewidth with that of the EIT feature.

feature [9]. The spectral position of the EIT feature is shifted from the coupling field by 4.8 MHz, corresponding to the frequency of the $|0,0\rangle\rightarrow|0,+1\rangle$ hyperfine transition, and the EIT feature has a spectral width determined by the linewidth of the hyperfine transition [9]. As stated previously, the width and position of the hyperfine transition varies under different static magnetic-field magnitude and alignment; however, there is always an excellent one-to-one correlation between relevant energies and linewidths of the hyperfine transition and the associated EIT feature. In addition to the sharp EIT feature, the coupling field changes the relative strength of the three broad ESR absorption lines. The changes in relative intensity are simply due to redistribution of the population among the hyperfine levels in the presence of the coupling field, a process similar to optical pumping. This effect is readily understood but is not followed in detail.

When a third rf field, the so-called driving field, is applied resonant with the $|0,0\rangle\rightarrow|0,-1\rangle$ hyperfine transition at 5.2 MHz, the EIT feature shown in Fig. 3 is split into two components (Fig. 4). The two components are of near equal intensity, and the magnitude of the splitting is linear in the strength of the driving field as shown in the left column of Fig. 4. When the driving field is detuned from the hyperfine transition resonance, one of the components gains intensity and moves to the position of the EIT feature in the absence of driving field, whereas the other component loses intensity and moves to lower or higher energy depending on the direction of detuning, as shown in the right column of Fig. 4.

The splitting of the EIT feature is achieved through driving a hyperfine transition, and would seem likely that the splitting is closely related to the dynamic ''Stark'' splitting (strictly speaking, to the dynamic Zeeman splitting as it is magnetic dipole transition involved) associated with the hyperfine transition. In the present experimental arrangement the dynamic Stark splitting of the hyperfine transition can be investigated directly, and the result is shown in Fig. 5. The figure presents a direct comparison between the dynamic Stark splitting of a hyperfine transition and the splitting of an EIT feature for a driving field resonant with the $|0,0\rangle\rightarrow|0,-1\rangle$ hyperfine transition at 5.2 MHz. The dynamic Stark splitting of the hyperfine transition is monitored by probing the $|0,0\rangle\rightarrow|0,+1\rangle$ hyperfine transition, whereas the splitting of EIT is probed as described above. It can be seen that there is an exact correspondence between the splitting of the EIT feature and the splitting of the hyperfine transition. The correspondence is maintained when the driving field is detuned. The splitting of the hyperfine transition and, therefore, of the EIT feature equals the Rabi or generalized Rabi frequency associated with the field driving the hyperfine transition.

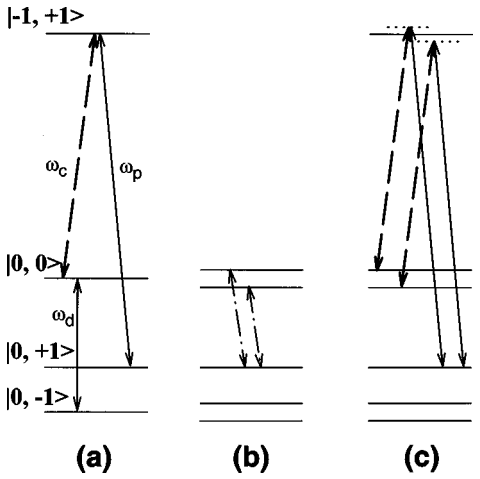

FIG. 6. Energy levels showing the configuration for observing the EIT splitting. (a) Gives bared-state energy levels and various applied fields. (b) Indicates the dressed-state levels when driving a hyperfine transition. The two transitions indicate the splitting of a hyperfine transition when probed to a separate (undriven) level as for a regular Autler-Townes spectrum. (c) Shows the transitions giving rise to the splitting of the EIT feature. The coupling field at fixed frequency is effective for two transitions and give two induced transparency features.

The splitting of the hyperfine transition as shown in Fig. 5 is simply an example of the well-known Autler-Townes spectrum which can be readily interpreted in terms of a dressed-state description of the total ''photon-atom'' system [19]. In the dressed-state model a strong field interacting with a transition gives rise to a ladder of degenerate states, and through the ''photon-atom'' interaction the degeneracy is lifted to give a ladder of doublets. The doublets are separated by the frequency of the driving field, and the splitting of the doublets is given by the associated Rabi frequency. In the case where the driving field is resonant with the $|0,0\rangle \rightarrow |0,-1\rangle$ hyperfine transition, the dressed-state levels are as given in Fig. 6. It is then seen that when probing the alternate hyperfine transition $|0,0\rangle \rightarrow |0,+1\rangle$, which has a shared level, the splitting is given by the Rabi frequency [Fig. 6(b)]. The same levels (plus one higher energy level) are involved with the EIT feature, and it can be readily seen why an equivalent splitting is observed. For example, from Fig. 6(c) it can be seen that levels associated with the coupling field are split by the Rabi frequency, and therefore the coupling field interacts with two transitions simultaneously. There will be an induced transparency when the frequency of the probing field matches the two photon resonance condition. Hence the single EIT feature is split into a doublet by the driving field (Figs. 4 and 5). The doublet splitting equals the Rabi frequency of the resonant driving field or the generalized Rabi frequency when the driving field is detuned from resonance. From this description it can be seen why the behavior of the EIT feature matches the characteristic of the related Autler-Townes spectrum.

From the dressed-state energy-level diagram, it can be anticipated that the driving field could be applied resonant with an alternative hyperfine transition, for example, at the frequency difference between the coupling and probing field. This creates a different situation to that described above, and is illustrated here using a second EIT spectrum. In this case

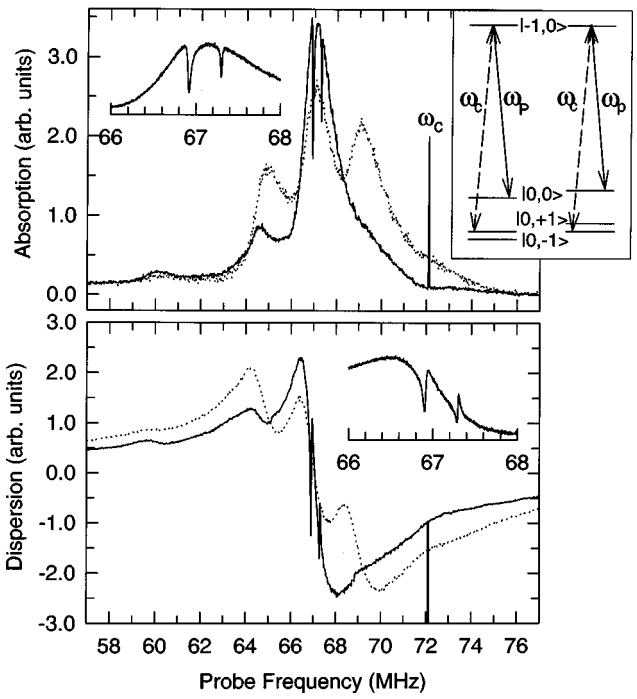

FIG. 7. ESR absorption and dispersion spectrum (dotted line) and EIT features (solid line) induced by applying a coupling field at 72.1 MHz as indicated by the pick-up peak. There are two EIT features shifted to lower energy by 4.8 and 5.2 MHz. The occurrence of two EIT features arises from the fact that due to inhomogeneous broadening the coupling field interacts with different subgroups of N-V centers with two alternate weak transitions: $|0,+1\rangle \rightarrow |-1,0\rangle$ and $|0,-1\rangle \rightarrow |-1,0\rangle$. The relevant energy levels and transitions are shown in the inset.

the EIT is obtained by applying a coupling field at the high-frequency side of the ESR transition. Due to the inhomogeneous broadening of the ESR transition, two EIT features are observed, associated with one coupling field, as shown in Fig. 7. For one subgroup of N-V centers the coupling field is resonant with the $|0,+1\rangle \rightarrow |-1,0\rangle$ transition, and introduces a transparency in the central ESR line. For another subgroup of N-V centers the coupling field is resonant with the $|0,-1\rangle \rightarrow |-1,0\rangle$ transition, and gives rise to another induced transparency feature in the central ESR line. In this way there are two EIT features in the ESR spectrum: one separated from the frequency of the coupling field by 5.2 MHz, and the other by 4.8 MHz.

To observe the splitting of the EIT features, an extra driving field is introduced resonant with one of the hyperfine transition $|0,0\rangle \rightarrow |0,+1\rangle$ at 4.8 MHz. For the EIT feature at the lower-energy side, only one of the three levels involved in the EIT is shared with the driven transition. This is an equivalent situation to that treated previously, and is consistent with the fact that the feature (shifted from coupling field by 5.2 MHz) is split into a doublet (Fig. 8). The splitting of the EIT feature at the high-energy side is different. In this case the feature is split into a triplet, with the separation between the components equal to the previous doublet splitting or the Rabi frequency of the driven field. In this case there are only three energy levels involved, and the triplet arises because there is a dynamic Stark splitting in both the coupled ($|0,+1\rangle \rightarrow |-1,0\rangle$) and probed ($|0,0\rangle \rightarrow |-1,0\rangle$)

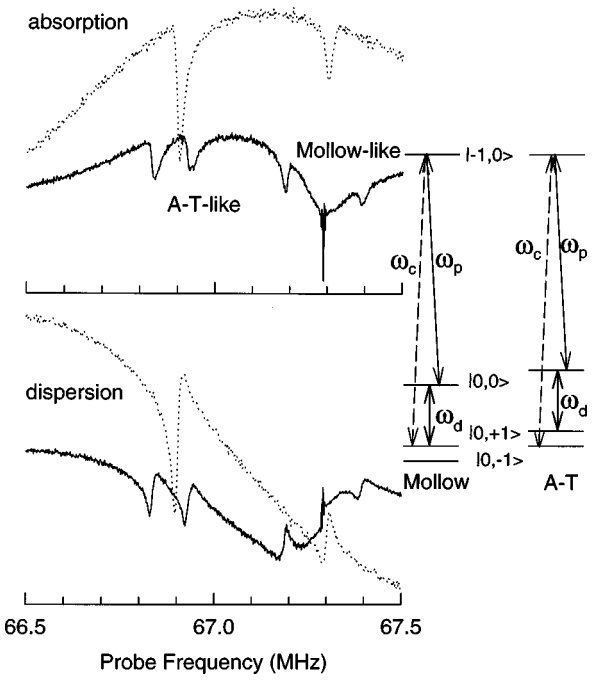

FIG. 8. Splitting of the EIT spectrum as given in Fig. 7 by a driving field at 4.8 MHz. The driving field Rabi frequency is 100 kHz. The EIT feature separated from the coupling field by 5.2 MHz at 66.9 MHz is split into a doublet (Autler-Townes type), whereas the EIT feature separated from the coupling field by 4.8 MHz at 67.3 MHz is split into a triplet (Mollow type).

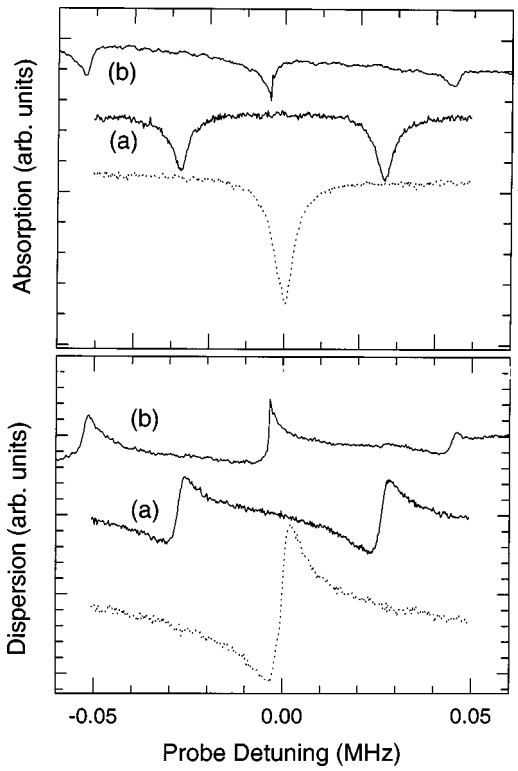

FIG. 9. Splitting of an EIT feature by the application of a driving field at the frequency of a hyperfine transition. The EIT in the absence of a driving field is given by the dashed trace. The feature is displaced from the coupling field by 5.2 MHz. The solid line gives the resultant EIT spectrum when a driving field is applied at (a) 4.8 MHz or (b) 5.2 MHz. In the text, (a) is described as being of Autler-Townes type, involving four levels, and (b) is described as being of Mollow type, involving only three levels.

transitions. There will be four possible EIT features; two are at the same frequency, resulting in the observed three line pattern.

For the previous configuration there was an equivalence between the observed EIT splitting and the Autler-Townes spectrum. In this second situation the equivalence is with a Mollow spectrum of a driven two-level atom. In the dressed-state description the driven two-level atom gives a ladder of doublets with four possible transitions between adjacent doublets. Two of these transitions are unshifted, and are equal in frequency to the frequency of the driving field. The other two transitions are displaced by the Rabi frequency to higher and lower frequencies. The result is a three-line pattern. There is a similarity with the splitting of the EIT feature, although clearly different intensities. When a two-level atom is probed directly, the magnitude of the absorption is quenched owing to an equalizing of the population of the two levels. The equalizing of the population does not have the same effect when the transition is probed via the splitting of the EIT feature. The outer components of the split EIT features are observed to have intensities almost equivalent to the original EIT feature. The central EIT feature in the current example is not so clear, and merits further investigation.

The pattern of the EIT splitting can be changed from a Mollow-type triplet to an Autler-Townes-type doublet by switching the driving field between the two hyperfine transitions at 4.8 and 5.2 MHz. This is shown for a single EIT feature in Fig. 9. The EIT feature in this instance is particularly clear, and was obtained using a different dc magnetic-field setting, and has a frequency shift of 5.2 MHz from the coupling field. When the 4.8-MHz hyperfine transition is driven, an Autler-Townes-type doublet is observed [Fig. 9(a)]. When the 5.2-MHz hyperfine transition is driven, a Mollow-type triplet is obtained [Fig. 9(b)]. The central component of the triplet in this instance is clearer than that obtained previously in Fig. 8, but the reason for this is not understood.

In principle the observed spectra can be calculated. The spectral positions of the split EIT features are readily anticipated, as the splitting and shift are simply related to the dynamic Stark splitting associated with the driven hyperfine transition. These are confirmed directly from parallel measurements of the dynamic Stark splitting of the hyperfine transitions, and there is a good agreement between experiment and calculation. The situation regarding the strengths (or depths) of the various EIT features is not so straightforward. For example, in the simplistic three-level atom without inhomogeneous broadening the transparency, for a sufficiently strong coupling field, can approach 100%, but this is not the case when there is inhomogeneous broadening. At any frequency there will be contributions from various centers, and these contributions can be estimated in the present system but will certainly reduce the depth of the transparency feature. Furthermore, the present system is a six-level system rather than three-level system and, thus, there can be other transitions overlapping the transition of interest. The pumping cycle will affect the background absorption upon which the EIT is superimposed, and this is another factor that is hard to reliably model as it requires knowledge of the

relaxation rates. Without such knowledge, modeling of the current EIT splitting, including inhomogeneously broadened six-level system, is not warranted. As an alternative we have undertaken a calculation of simpler cases. We consider homogeneously broadened three- and four-level systems similar to the situation considered in Ref. [20]. When the Rabi frequency of the driving field is strong compared to the hyperfine transition linewidth, but weak compared to the ESR linewidth, the calculations give spectra with reasonable correlation with present observations. When the strength of the driving field or coupling field is large compared to the ESR linewidth, very different patterns are predicted. However, such strengths cannot be realized in the current experimental setup, and it would no longer be valid to model the present six-level system with three or four levels. As such situations have not been achieved experimentally, we prefer to report the details of these calculations including the more extensive driving configuration in separate papers. In this paper we rely on a semiquantitative analysis using the dressed-state model.

The calculations and the dressed-state analysis confirm that the EIT splitting arises from dynamic Stark effect. The dynamic Stark effect was originally observed for transitions associated with real atomic levels, and it is of interest to see that the EIT feature exhibits a similar behavior even though the spectral features are associated with quantum interference processes rather than absorption. Our present observations show that the EIT feature can be modified in a similar way to that of an atomic transition, including splitting and shifting of the spectral feature. The extra driving field provides a way of manipulating the EIT feature, such as opening a multi-EIT window, frequency tuning the EIT, or changing the refractive index. Although the present effects are observed in the radio-frequency region of the spectrum, the physics is applicable to any frequency, and there are many real atomic systems with more than two sublevels. The work may, therefore, stimulate interest in experiments in optical frequency region, where the effects hold more promise in technical applications.

IV. SUMMARY

In this paper we studied EIT and its response to a strong driving field using a unique experimental system including a sensitive coherent detection technique and a controllable energy-level structure. We observed both doublet and triplet splittings of the EIT feature. The splitting is shown to correspond very well to the Autler-Townes doublet and Mollow triplet observed in real atomic transitions and originates from the dynamic Stark effect.

[1] For recent review articles, see J. P. Marangos, J. Mod. Opt. **45**, 471 (1998); E. Arimondo, Prog. Opt. **35**, 257 (1996).

[2] E. Arimondo and G. Orriols, Lett. Nuovo Cimento **17**, 333 (1976); G. Alzetta, A. Gozzini, L. Moi, and G. Orriols, Nuovo Cimento B **36**, 5 (1976); G. Alzetta, L. Moi, and G. Orriols, *ibid.* **52**, 209 (1979); , **53**, 1 (1979).

[3] H. R. Gray, R. M. Whitley, and C. R. Stroud, Jr., Opt. Lett. **3**, 218 (1978).

[4] K. J. Boller, A. Imamoglu, and S. E. Harris, Phys. Rev. Lett. **66**, 2593 (1991); J. E. Field, K. H. Hahn, and S. E. Harris, *ibid*. **67**, 3062 (1991).

[5] M. Xiao, Y. Li, S. Jin, and J. Gea-Banacloche, Phys. Rev. Lett. **74**, 666 (1995); Y. Li and M. Xiao, Phys. Rev. A **51**, R2703 (1995); **51**, 4959 (1995); J. Gea-Banacloche, Y. Li, S. Jin, and M. Xiao, *ibid*. **51**, 576 (1995).

[6] R. R. Moseley, S. Shepherd, D. J. Fulton, B. D. Sinclair, and M. H. Dunn, Phys. Rev. Lett. **74**, 670 (1995); J. R. Boon, E. Zekou, D. J. Fulton, and M. H. Dunn, Phys. Rev. A **57**, 1323 (1998).

[7] D. J. Fulton, S. Shepherd, R. R. Moseley, B. D. Sinclair, and M. Dunn, Phys. Rev. A **52**, 2302 (1995).

[8] R. Rakhmatullin, E. Hoffmann, G. Jeschke, and A. Schweiger, Phys. Rev. A **57**, 3775 (1998).

[9] C. Wei and N. B. Manson, J. Opt. B. Quantum Semiclassic. Opt. (to be published).

[10] J. Mlynek, N. C. Wong, R. G. DeVoe, E. S. Kintzer, and R. G. Brewer, Phys. Rev. Lett. **50**, 993 (1983); N. C. Wong, E. S. Kintzer, J. Mlynek, R. G. DeVoe, and R. G. Brewer, Phys. Rev. B **28**, 4993 (1983).

[11] K. Holliday, N. B. Manson, M. Glasbeek, and E. van Oort, J. Phys.: Condens. Matter **1**, 7093 (1989).

[12] C. Wei, S. A. Holmstrom, N. B. Manson, J. P. D. Martin, X.-F. He, P. T. H. Fisk, and K. Holliday, Appl. Magn. Reson. **11**, 521 (1996); C. Wei, S. A. Holmstrom, N. B. Manson, and J. P. D. Martin, *ibid*. **11**, 539 (1996).

[13] C. Wei and N. B. Manson, Phys. Rev. A **49**, 4751 (1994).

[14] C. Wei, J. P. D. Martin, and N. B. Manson, Phys. Rev. A **51**, 1438 (1995).

[15] B. R. Mollow, Phys. Rev. **188**, 1969 (1969); **5**, 2217 (1972); F. Y. Wu, R. E. Grove, and S. Ezekiel, Phys. Rev. Lett. **35**, 1426 (1975); F. Y. Wu, S. Ezekiel, M. Ducloy, and B. R. Mollow, *ibid*. **38**, 1077 (1977).

[16] S. H. Autler and C. H. Townes, Phys. Rev. **100**, 703 (1955).

[17] G. Davies and M. F. Hamer, Proc. R. Soc. London, Ser. A **348**, 285 (1976); J. H. N. Loubser and J. A. van Wyk, Rep. Prog. Phys. **41**, 1201 (1978).

[18] N. R. S. Reddy, N. B. Manson, and E. R. Krausz, J. Lumin. **38**, 46 (1987).

[19] C. Cohen-Tannoudji and S. Reynaud, J. Phys. B **10**, 345 (1977); **10**, 365 (1977); **10**, 2311 (1977); C. Cohen-Tannoudji, J. Dupont-Roc, and G. Grynberg, *Atoms-Photon Interactions: Basic Processes and Applications* (Wiley, New York, 1992).

[20] J. C. Petch, C. H. Keitel, P. L. Knight, and J. P. Marangos, Phys. Rev. A **53**, 543 (1996); C. H. Keitel, *ibid*. **57**, 1412 (1998).